Received: 14 September 2018 | Revised: 19 November 2018 | Accepted: 23 November 2018

DOI: 10.1002/aoc.4770

FULL PAPER

WILEY Applied Organometallic Chemistry

Homoleptic, bis-ligated magnesium complexes for ring-opening polymerization of lactide and lactones: Synthesis, structure, polymerization behavior and mechanism studies

Xiao-Lu Chen[1] | Bin Wang[1] | Li Pan[1] | Yue-Sheng Li[1,2]

[1]Tianjin Key Lab of Composite and Functional Materials, School of Materials Science and Engineering, Tianjin University, Tianjin 300072, China

[2]Collaborative Innovation Center of Chemical Science and Engineering (Tianjin), Tianjin 300072, China

Correspondence
Bin Wang, Tianjin Key Lab of Composite and Functional Materials, School of Materials Science and Engineering, Tianjin University, Tianjin 300072, China.
Email: binwang@tju.edu.cn

Funding information
National Natural Science Foundation of China, Grant/Award Number: 21474100

Bis-ligated, homoleptic magnesium complexes **1–3** were synthesized through the reaction of 1 equiv. dibutyl magnesium with 2 equiv. *β*-ketiminato ligands bearing different substituents on the nitrogen atom and 8 position on benzocyclohexanone. All of the complexes were identified by nuclear magnetic resonance (NMR) and X-ray crystallography. Complexes **2** and **3** adopted distorted tetrahedral geometry around Mg, by chelating of two ancillary ligands, while complex **1** adopted a dimeric structure with penta-coordination around Mg. These complexes can be used as efficient catalysts for the ring-opening polymerization of *L*-lactide, *ε*-caprolactone, *δ*-valerolactone (*δ*-VL) and trimethylene carbonate in the presence of alcohol as a co-initiator. With the increasing steric bulk of the ancillary ligands, the catalytic activity of Mg complexes was improved significantly. Particularly, complex **3** having the largest steric hindrance showed excellent catalytic performance for the polymerization of *δ*-VL. It could polymerize 800 equiv. *δ*-VL in 10 min, and produce polyvalerolactone with narrow molecular weight distributions ($M_w/M_n < 1.2$) at 35°C or higher temperature. No transesterification side reaction was observed. Moreover, complex **3** exhibited good tolerance to excessive alcohol and an immortal polymerization characteristic. The mechanism studies by *in situ* NMR demonstrated a coordination-insertion process. Besides, it revealed that the steric bulky substituents in the active species derived from the complex and alcohol prevented the metal center from deactivation.

KEYWORDS
bis-ligated, magnesium complex, polyester, ring-opening polymerization, *δ*-valerolactone

1 | INTRODUCTION

Over recent decades, biodegradable polymers have been widely applied in the biomedical field and industries because of their particular and remarkable biodegradability and biocompatibility.[1–3] Therefore, fundamental research on the synthesis of aliphatic polyester, which is an important biodegradable polymer, has attracted attention and developed rapidly.[4–6] Ring-opening polymerization (ROP) initiated by organometallic catalysts is one of the most effective methods to synthesize polyester-like polylactide (PLA), polycaprolactone (PCL) and other polyesters with high molecular weight (MW) and narrow

Electronic supplementary information (ESI) available: characterization of ligand and binuclear complex, crystal data and structure refinements of complexes **1–3**, and crystallographic data in CIF format. CCDC: 1855155 for **1**, 1855633 for **2** and 1855636 for **3**.

molecular weight distribution (MWD).[7–12] A variety of complexes with different metal centers have been studied and proved to be effective catalysts. As it is hard to remove metallic residues in polymers completely, the resultant polyesters initiated by the complexes of toxic metals such as tin and aluminum may have negative effects on the human body, causing their limited application in the field of green packaging and medical devices.[13–17] At this point, the catalysts with non-toxic and biologically benign metals like magnesium,[18–26] zinc,[27–33] calcium[26] and iron[34] are more suitable and superior catalysts.[35,36]

In most organometallic complexes of divalent metals such as magnesium and zinc for the ROP of cyclic esters, the metal centers are supported by a multi-dentate ligand and the complexes are formed as type of LM-X [where X = Et, OBn, $OSiPh_3$, O^tBu_2Ph, N $(SiMe_3)_2$ or NPr_2].[37,38] Generally, the efficient catalysts for the ROP of cyclic esters were reported to be these heteroleptic complexes (LM-X). They are always more reactive than the corresponding homoleptic complexes, because of the difference in electron unsaturation and Lewis acidity of the magnesium center.[37,39–41] Most of the bis-chelated complexes ML_2 were inactive or exhibited negligible activity, sometimes because of their poor solubility.[41–46]

However, previous reports showed that some homoleptic complexes were indeed active in ROP of cyclic esters in the presence of external alcohol (Scheme 1).[10,13,37,40,47–49] The Ejfler group developed a kind of hetero- and homoleptic molecular zinc complexes with one or two equivalents of aminophenolate ligand in 2008 (Scheme 1a).[40] In 2014, Gerling *et al*. reported bis-ligated zinc complexes, which could catalyze the ROP of *L*-lactide (*L*-LA) at high temperature with a more acidic phenol as an initiator (Scheme 1b).[37] Nonetheless, the transesterification was still detected and hard to be eliminated, leading to the uncontrolled polymerization process. The homoleptic zinc and magnesium complexes synthesized by the Ejfler group in 2014 showed high efficiency for ROP of *L*-LA at 58°C, which completed the polymerization almost in 15 min (Scheme 1c).[13] The Dagorne group reported that the homoleptic bis (phosphinophenolate) Zn (II) complex (Scheme 1d) in combination with BnOH initiated the ROP of 100 equiv. *rac*-LA at room temperature via an 'activated monomer' mechanism.[39] To initiate the polymerization effectively, it was necessary to feed rather a high ratio of catalyst (over 1/50 equiv. to monomer), and the resultant PLA showed low MW. The homoleptic zinc complex (Scheme 1e) based on salicylaldiminato ligands synthesized by the Wu group needed to be activated by raising the temperature to 130°C.[47] Some homoleptic magnesium complexes (Scheme 1f–h) produced PCLs in 15–60 min, with MWs diverging from theoretical MWs or broad MWD.[10,48,49] Though the homoleptic metal complexes were not traditionally regarded as effective initiators for ROP of cyclic esters, these elegant studies showed that the homoleptic, bis-ligated organometallic complexes can be a potentially effective catalytic system in ROP of lactides and lactones, especially in the presence of external alcohol. As aforementioned, previous reported monomers initiated by homoleptic complexes were mainly LA and ε-caprolactone (ε-CL). ROP of other cyclic esters was seldom reported.

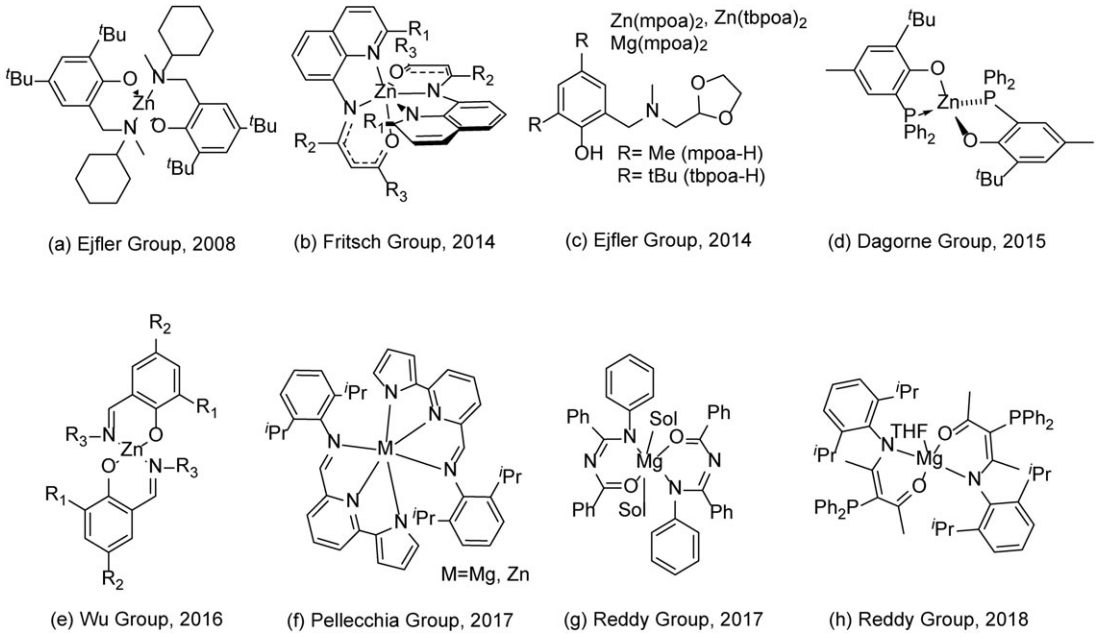

SCHEME 1 The typical homoleptic, bis-ligated organometallic complexes

Herein, we synthesized a series of magnesium bis (chelate) complexes supported by two bidentate cyclic β-ketiminato ligands with different substituents attaching to the nitrogen atom and the 8 position on benzocyclohexanone (Scheme 2). They were found to be a kind of effective catalytic system in the ROP of lactides and lactones, combining with benzyl alcohol (BnOH) and isopropyl alcohol (^{i}PrOH). Among them, the catalytic system composed of complex **3** and alcohol displayed promising performance for ROP of various monomers, including *L*-LA, ε-CL, δ-valerolactone (δ-VL) and trimethylene carbonate (TMC) under mild conditions, showing living and controlled nature. These homoleptic L_2Mg complexes were not stable in the presence of external alcohol, and the real catalytic species were presumed to be heteroleptic LMgOR complexes obtained by *in situ* alcoholysis.

2 | RESULTS AND DISCUSSION

2.1 | Synthesis and characterization of bis-ligated magnesium complexes

Cyclic β-ketiminato proligands with different substituents (**L^1H–L^3H**) were prepared according to the literature methods.[50] The structures of the resultant proligands were characterized spectroscopically and crystallographically. Complexes **1–3** were synthesized by the reaction of Mg^{n}Bu$_2$ (2 M in heptane) and 2 equiv. ligands **L^1H–L^3H**, and were characterized clearly by ^{1}H-nuclear magnetic resonance (NMR), ^{13}C-NMR spectra and elemental analysis (see Figures S1–S3 of ESI). In the ^{1}H-NMR spectra, the proton resonances of the Mg complex exhibit apparent chemical shifts from those of the corresponding proligands. Compared with proligand **L^3H**, the proton resonances of methyl groups in 2,6-^{i}Pr$_2$C$_6$H$_3$ belonging to complex **3** split into four doublets, suggesting that methyl groups become chemically inequivalent after coordination with magnesium atom. The broad singlet peaks at $\delta \sim 11.3$ ppm corresponding to the exchangeable proton (-OH) in the ketiminato ligands disappear. Additionally, there are no signals of the *n*-butyl protons bound to the magnesium metal center in the upfield region. The successful coordination of the ligands with magnesium and formation of bis (chelate) complexes are confirmed by the NMR spectroscopic data and elemental analyses. Single crystals of complexes **1–3** suitable for X-ray crystallographic analysis were prepared via the diffusion of hexanes into a toluene solution at ambient temperature. Crystallographic and refinement data are summarized in Table S1 (see ESI), and the selected bond lengths and angles are listed in Table 1.

The magnesium atoms in complexes **2** and **3** are coordinated with two bidentate N,O-ligands, adopting a monomeric structure with distorted tetrahedral geometry around Mg. In contrast, complex **1** adopts a dimeric structure (Figure 1; Figures S4 and S5 of ESI), in which two magnesium centers are penta-coordinated with four bidentate N,O-ligands symmetrically and bridged via the oxygen atoms of the ketiminato ligands. The formation of dimer is ascribed to the low steric hindrance of the proligand **L^1**. Complexes **2** and **3** have very similar Mg-O bond lengths. The lengths of Mg1-O1 and Mg1-O2 are 1.9185(15) and 1.9174(16) Å for complex **2**, and 1.9260(9) and 1.9260(9) Å for complex **3**, respectively. The bond length values are in the normal range of Mg–O bond lengths (generally ranging from 1.889 to 1.999 Å).[24,51] The bond lengths between magnesium and nitrogen (Mg1-N1, Mg1-N2) in complex **3** [2.0511(11)

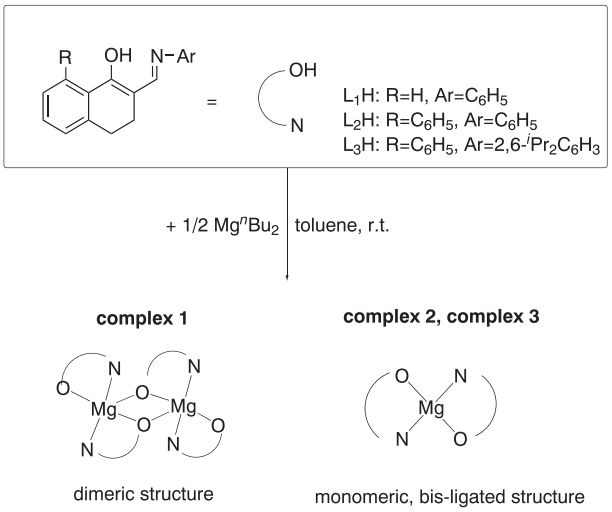

SCHEME 2 Synthesis of complexes **1–3**

TABLE 1 Selected bond lengths and angles in complexes **1–3**

	1	2	3
Bond lengths in Å			
Mg1-N1	2.1165(12)	2.0852(18)	2.0511(11)
Mg1–N2	2.1302(12)	2.0705(18)	2.0511(11)
Mg1–O1	2.0268(10)	1.9185(15)	1.9260(9)
Mg1–O2	2.0344(10)	1.9174(16)	1.9260(9)
Bond angles in °			
O1–Mg1–N1	97.73(4)	104.63(7)	114.41(4)
O1–Mg1–N2	113.64(4)	89.53(7)	90.32(4)
O2–Mg1–O1	173.16(4)	134.90(8)	121.54(6)
O2–Mg1–N1	87.50(4)	89.22(7)	90.32(4)
O2–Mg1–N2	89.54(4)	104.90(7)	114.41(4)
N2–Mg1–N1	127.26(5)	142.91(8)	129.20(7)

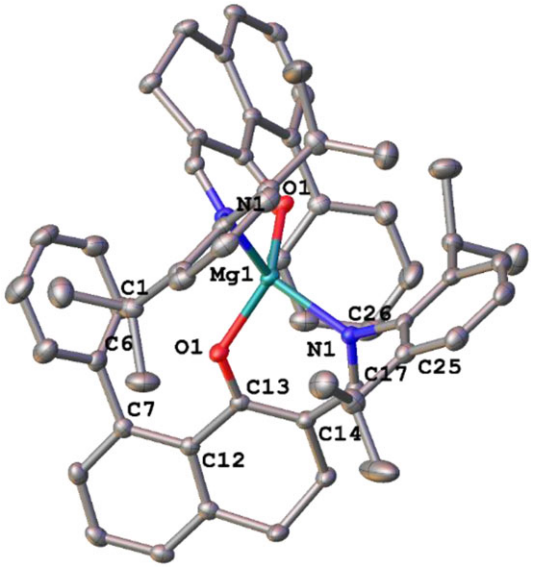

FIGURE 1 ORTEP drawing of complex **3** with thermal ellipsoids at the 30% probability level. Hydrogen atoms have been omitted for clarity

and 2.0511(11) Å] are a little shorter than those of complex **2** [2.0852(18) and 2.0705(18) Å]. Additionally, the Mg-N and Mg-O bonds in complex **1** are the longest [Mg1-N1, Mg1-N2, Mg1-O1, Mg1-O2 are 2.1165(12), 2.1302(12), 2.0268(10), 2.0344(10) Å, respectively]. This implies the possible stronger coordination of magnesium atom with nitrogen atom from $\mathbf{L}^3$ and the loose coordination around the magnesium atom in complex **1**, on account of the dimeric nature of complex **1** where each magnesium center is penta-coordinated.

Without any substituents in the 8 position of the phenyl ring and aromatic amine moiety of *β*-ketiminato ligands in complex **1**, the least steric hindrance leads to the dimeric behavior. In complex **1**, the angle between O2–Mg1–O1 is 173.16(4), while the angles in complexes **2** and **3** are 134.90(8) and 121.54(6), respectively. This demonstrates that the magnesium center is nearly coplanar with these two O atoms in comlex 1. Without protection from the steric hindrance of the bis-chelated bidentate proligands, it is liable to be attacked and inactivated. The six-membered Mg-O-C-C-C-N ring is nearly planar in complexes **1** and **2**, but is more distorted in complex **3**. The torsion angles around the magnesium center for **1** (Mg-N1-C7-C8), **2** and **3** (Mg-N1-C17-C14) are 9.8°, 8.9° and −12.5°, respectively. The dihedral angles between the aromatic moieties bonding to the nitrogen atom and the six-membered ring are −58.9° in complex **1** (C7-N1-C6-C5), 50.9° in complex **2** (C40-N1-C41-C42) and −81.63° in complex **3** (C17-N1-C26-C25). The aromatic ring linked with the nitrogen atom in complex **3** is much more tilted and nearly perpendicular to the organometallic skeleton. These results indicate that the large steric bulk of the substituents in complex **3** makes the space around the magnesium center crowded and 2,6-^{i}Pr$_2$C$_6$H$_3$ groups difficult to rotate. The steric bulk around the metal center is able to prevent complex **3** from deactivation by protons and transesterification side reaction in the ROP process, which is going to be investigated further in the mechanism study.

2.2 | ROP of lactides and lactones by complexes 1–3

Combined with ^{i}PrOH and BnOH, the homoleptic complexes were proved to be effective catalysts for ROP of *L*-LA, *ε*-CL, *δ*-VL and TMC. All of the polymerizations were explored at 80°C or 35°C in the presence of ^{i}PrOH or BnOH (1 equiv. to Mg complex), and the typical results were summarized in Table 2. Complexes **1**–**3** were able to polymerize *L*-LA, *ε*-CL and *δ*-VL effectively, achieving high monomer conversion easily in 1 hr under optimized conditions.

Complexes **1** and **2** showed no activity in ROP of *L*-LA and *ε*-CL at 35°C in the presence of BnOH (Table 2, entries 1, 3, 8 and 10). However, when increasing the temperature to 80°C, they were able to polymerize *L*-LA and *ε*-CL rapidly (Table 2, entries 2, 4, 9 and 11). The conversion initiated by complex **1** was up to 92% in 1 hr, producing PLA with moderate MW (M_n = 24.2 kDa) and narrow MWD (M_w/M_n = 1.12; Table 2, entry 2). The experimental MW was consistent with the theoretical MW well, indicating the controlled performance in ROP of *L*-LA. However, the resultant PCL produced by complexes **1** and **2** had much lower experimental MW (M_n = 4.67 and 10.4 kDa) with relatively broad MWD (M_w/M_n = 1.34 and 1.36) compared with theoretical values (Table 2, entries 4 and 11). Here, we hypothesized that there may be depolymerization, transesterification and accelerated chain transfer in the ROP of *ε*-CL at high temperature. Interestingly, complex **1** can prompt the ROP of *δ*-VL at 35°C in the presence of ^{i}PrOH or BnOH. Compared with ^{i}PrOH, BnOH can activate complex **1** more effectively (Table 2, entry 5 vs. 6). The structure of the alcohol had great influence on ROP of *δ*-VL initiated by complex **1**. The conversion was 49% in 1 hr with the co-initiation of BnOH at 35°C, while it was 29% with ^{i}PrOH, producing PVL with M_n = 7.31 kDa. In the ROP of *δ*-VL, complex **2** showed much higher activity than complex **1** and was less dependent on alcohol co-initiator. It could initiate the ROP of 400 equiv. *δ*-VL at mild conditions and the monomer conversion was 69% and 62% with ^{i}PrOH and BnOH, respectively (Table 2, entries 12 and 13).

The deviation between the experimental MW and calculated MW was observed in ROP of *ε*-CL and *δ*-VL

TABLE 2 ROP of lactides and lactones catalyzed by complex **1–3**/ROH system[a]

Entry	Complex	Monomer	ROH	T (°C)	[M]/[I]/ROH	t (min)	Conv.[b] (%)	$M_{n,calcd}$[c] ($\times 10^3$)	M_n[d] ($\times 10^3$)	M_w/M_n[d]
1	**1**	*L*-LA	BnOH	35	200/1/1	60	trace	–	–	–
2	**1**	*L*-LA	BnOH	80	200/1/1	60	92	26.5	24.2	1.12
3	**1**	ε-CL	BnOH	35	200/1/1	60	trace	–	–	–
4	**1**	ε-CL	BnOH	80	200/1/1	60	92	21.0	4.67	1.34
5	**1**	δ-VL	^{i}PrOH	35	400/1/1	60	29	11.6	n.d.	n.d.
6	**1**	δ-VL	BnOH	35	400/1/1	60	49	19.6	7.31	1.22
7	**1**	δ-VL	^{i}PrOH	80	400/1/1	60	88	35.2	6.18	1.37
8	**2**	*L*-LA	BnOH	35	200/1/1	60	trace	–	–	–
9	**2**	*L*-LA	BnOH	80	200/1/1	60	> 99	28.8	33.2	1.26
10	**2**	ε-CL	BnOH	35	200/1/1	60	trace	–	–	–
11	**2**	ε-CL	BnOH	80	200/1/1	60	94	21.5	10.4	1.36
12	**2**	δ-VL	^{i}PrOH	35	400/1/1	60	69	27.6	8.68	1.52
13	**2**	δ-VL	BnOH	35	400/1/1	60	62	24.8	13.3	1.54
14	**3**	*L*-LA	BnOH	35	200/1/1	60	78	22.5	28.3	1.17
15	**3**	*L*-LA	^{i}PrOH	35	400/1/1	60	65	37.5	33.3	1.11
16	**3**	ε-CL	BnOH	35	200/1/1	10	97	22.1	20.3	1.09
17	**3**	ε-CL	^{i}PrOH	35	400/1/1	10	66	30.1	30.2	1.07
18	**3**	δ-VL	^{i}PrOH	35	400/1/1	10	94	37.6	28.7	1.11
19	**3**	δ-VL	BnOH	35	400/1/1	10	93	37.2	31.4	1.09
20	**3**	TMC	^{i}PrOH	35	400/1/1	10	88	35.9	10.7	1.39

[a]All reactions were conducted in toluene at 80°C or 35°C, $[M]_0 = 1.0$ M.

[b]Monomer conversions were calculated by ^{1}HNMR.

[c]Calculated by $([Mono.]_0/[OH]_0) \times M_w$ (Mono.) × conv. (%) + M_w (^{i}PrOH) or M_w (BnOH).

[d]Determined by GPC analysis (THF).

catalyzed by complexes **1** and **2**. According to the coordination-insertion mechanism, the metal center at the end of the active chain can attack not only the carbonyl groups of the monomers but also those of active chains, causing transesterification and depolymerization.[9] It is assumed that complexes **1** and **2**, with less steric hindrance and weak protection around the metal center, can polymerize the lactones and depolymerize the polymer at the same time. At 80°C, complex **1** could polymerize 400 equiv. δ-VL in 1 hr and the conversion was up to 88% (Table 2, entry 7), giving PVL with MW = 6.18 kDa. The significant divergence of experimental M_n from the theoretical value ($M_{n,calcd}$ = 35.2 kDa) indicated chain transfer and depolymerization reaction under higher temperature. To prove the transesterification or the depolymerization reaction in complex **1**, a sequential copolymerization of 200 equiv. ε-CL first and then 200 equiv. δ-VL was further conducted by 1 equiv. complex **1** at 80°C. The resultant copolymer was analyzed by ^{13}C-NMR (Figure S6a). Four resonance peaks corresponding to CL-CL, VL-VL, VL-CL and CL-VL, respectively, were clearly detected, which confirmed the depolymerization and transesterification reaction in the ROP of CL catalyzed by complex **1**. By sharp contrast, the majority of continuous CL-CL and VL-VL of homodyads and a very small fraction of VL-CL and CL-VL heterodyads were observed in the copolymer obtained by complex **3** (Figure S6b). Apparently, complex **3** with the largest steric bulk showed superior catalytic performances for ROP of *L*-LA, ε-CL and δ-VL at mild conditions. Complex **3** was able to polymerize 200 equiv. *L*-LA at 35°C and the monomer conversion was up to 78% in 1 hr, while complexes **1** and **2** did not exhibit satisfying activity under the same conditions (Table 2, entries 1, 8 and 14). Compared with the reported bis-ligated complexes, where higher temperature (70°C, 100°C or 130°C) or catalyst loading (monomer/catalyst = 50/1) were necessary, complex **3** with the highest activity was able to polymerize 200–400 equiv. *L*-LA in 60 min and ε-CL in 10 min at 35°C, giving PLAs and PCLs with moderate MW (M_n = 20–35 kDa) and narrow MWD ($M_w/M_n < 1.2$).

It was noted that complex **3** also displayed excellent activity for ROP of δ-VL, which can convert 400 equiv. monomers in 10 min at 35°C in the presence of ^{i}PrOH or BnOH (Table 2, entries 16–19). The polymerization rate was rather fast compared with the reported N-heterocyclic olefins (NHOs)/Lewis acid pairs, which polymerize 100 equiv. δ-VL in 80 min,[52] and the M_w/M_n was still less than 1.1. In addition, complex **3** could polymerize 400 equiv. TMC almost completely in 10 min, affording PTMC with relatively higher M_w/M_n (Table 2, entry 20). Taking all of the results into account, it clearly demonstrated that complex **3** possessed the highest activity in the ROP of *L*-LA and other lactones. With the increasing steric bulk of the substituent in the ligands, the catalytic performance of the complexes enhanced significantly. Moreover, the catalytic activity of complex **1** was highly dependent on the structure of the co-initiator, while no significant difference in catalytic activity was observed for complex **3** by using different alcohols. We envisioned that the bulky steric hindrance in active species protected the central magnesium from deactivation and improved the stability of active species during the polymerization process. We will give a detailed discussion later.

2.3 | ROP of δ-VL catalyzed by complex 3

There have been lots of investigation about the ROP of ε-CL, and a lack of study on the ROP of δ-VL,[8,53] which was a six-membered ring and had lower polymerization reactivity than ε-CL with a structure of a seven-membered ring. As complex **3** showed outstanding activity in ROP of δ-VL, polymerization under different conditions was studied in detail. The typical results were summarized in Table 3. In most of the experiments, the conversion reached up to 90% rapidly with the co-initiation of ^{i}PrOH or BnOH, affording polyvalerolactone (PVL) with consistently narrow polydispersity. Complex **3** was capable of completing the polymerization of 800 equiv. δ-VL in 10 min in toluene solution ($M_0 = 2.0$ M) under mild conditions (Table 3, entries 8 and 9). Increasing the temperature resulted in the decrease of MW notably, which might be ascribed to the more rapid chain transfer (Table 3, entry 1 vs. 3, 2 vs. 4). The MW increased with a higher monomer feed ratio (Table 3, entry 3 vs. 6, 4 vs. 7, 9 vs. 10). For example, complex **3** can polymerize 1000 equiv. δ-VL and afford PVL with M_n = 76.2 kDa, while it produced PVL with M_n = 42.0 kDa when feeding 800 equiv. δ-VL (Table 3, entry 9 vs. 10). The experimental MWs were relatively lower than the calculated MWs. This divergence may be ascribed to the presence of trace impurities as other chain transfer agents (CTAs). The trace impurities might have more influence and make the divergences more serious when less catalyst was fed.[54] At high catalyst loading (the monomer to catalyst ratio was under 400/1), the experimental MWs matched better with the calculated values than at lower catalyst loading (Table 3, entries 4 and 7). Besides, when the loading of ROH was higher, the MWs were closer to the theoretical MW (Table 4), in agreement with the previous

TABLE 3 ROP of δ-VL catalyzed by complex **3**/ROH system[a]

Entry	ROH	*T*(°C)	[M]/[I]/ROH	Time (min)	Conv.[b] (%)	$M_{n,calcd}$[c] (× 10^3)	M_n[d] (× 10^3)	M_w/M_n[d]
1	^{i}PrOH	80	200/1/1	60	91	18.2	4.52[f]	1.03[f]
2	^{i}PrOH	50	400/1/1	10	94	37.6	22.0	1.14
3	^{i}PrOH	35	200/1/1	60	92	18.4	10.2	1.10
4	^{i}PrOH	35	400/1/1	10	94	37.6	28.7	1.11
5	BnOH	35	400/1/1	10	93	37.2	31.4	1.09
6	^{i}PrOH	35	800/1/1	60	93	74.5	37.5	1.09
7	^{i}PrOH	35	800/1/1	10	78	62.4	37.6	1.14
8[e]	^{i}PrOH	35	800/1/1	10	96	76.9	40.6	1.13
9[e]	BnOH	35	800/1/1	10	90	72.1	42.0	1.12
10[e]	BnOH	35	1000/1/1	20	83	83.1	76.2	1.27

[a]All reactions were conducted in toluene at 35°C, where $[M]_0 = 1.0$ M.

[b]Monomer conversions were measured by ^{1}H-NMR.

[c]Calculated by $([VL]_0/[OH]_0) \times M_w$ (VL) × conv. (%) + M_w (^{i}PrOH) or M_w (BnOH).

[d]Determined by GPC analysis (THF).

[e]Polymerization condition: $[M]_0 = 2.0$ M.

[f]The obtained polyester was tested by MALDI-TOF MS.

TABLE 4 ROP of δ-VL catalyzed by complex **3** with excessive alcohol[a]

Entry	ROH	[M]/[I]/ROH	Time (min)	Conv.[b] (%)	$M_{n,calcd}$[c] ($\times 10^3$)	M_n[d] ($\times 10^3$)	M_w/M_n[d]
1	^{i}PrOH	800/1/5	10	96	15.4	10.4	1.15
2	^{i}PrOH	800/1/10	10	85	6.87	7.13	1.11
3	^{i}PrOH	800/1/20	10	95	3.80	4.8	1.17
4	BnOH	800/1/5	5	64	10.3	14.3	1.06
5	BnOH	800/1/10	10	88	7.05	7.44	1.10
6	BnOH	800/1/20	10	95	3.91	4.33	1.09
7	BnOH	1000/1/50	20	94	1.99	2.70[e]	1.02[e]

[a]All reactions were conducted in toluene at 35°C, where $[M]_0 = 2.0$ M.

[b]Monomer conversions were measured by ^{1}H-NMR.

[c]Calculated by $([VL]_0/[OH]_0) \times M_w$ (VL) × conv. (%) + M_w (^{i}PrOH) or M_w (BnOH).

[d]Determined by GPC analysis (THF).

[e]The obtained polyester was detected by MALDI-TOF MS.

literature.[54] It was ascribed to the higher reactivity of ROH or the polymeric alcohol in the transfer and exchange than other impurities functioned as CTAs.[53]

As the ROP of δ-VL cannot proceed smoothly without alcohol as co-initiator, the alcohol plays a significant role in the initiation of polymerization. The effect of alcohol loading content was also investigated, and the results were displayed in Table 4. Most of the heteroleptic organometallic complexes were sensitive to the excess of external alcohol.[10,13] However, complex **3** still exhibited high catalytic activity when the ROH/Mg ratio varied from 5 to 50, with monomer conversion up to 90% in 10 min. The molecular weight of PVLs was basically proportional to the amount of ROH. This result showed an immortal nature of the complex **3**/ROH catalytic system in ROP of δ-VL, where each magnesium metal center could initiate at most 50 PVL chains with overloading of ROH. The narrow MWD confirmed the reversible and fast chain transfer caused by the excessive ROH as CTA. In addition, a linear relationship between M_n and monomer conversion was found with consistently narrow MWD (see Figure S7 of ESI). This ensured the living and controlled nature of this binary catalytic system composed of the magnesium complex **3** and alcohol. The kinetics study was conducted in toluene in the presence of ^{i}PrOH at 35°C with [VL] = 1.0 M and [M] = [I] = 1.25 mM. The polymerization reaction was found to be first-order dependent on the monomer concentration with an apparent rate constant of 0.135 min^{-1} (see Figure S8 of ESI).

The structures of PVLs produced by complex **3**/ROH were characterized by ^{1}H-NMR and MALDI-TOF MS (Figure 2, and Figures S9 and S10 of ESI). In the ^{1}H-NMR spectra (see Figure S9 of ESI), the corresponding resonance peaks assigned to the methene group in the terminal hydroxyl part (peak e in Figure S9), the methene

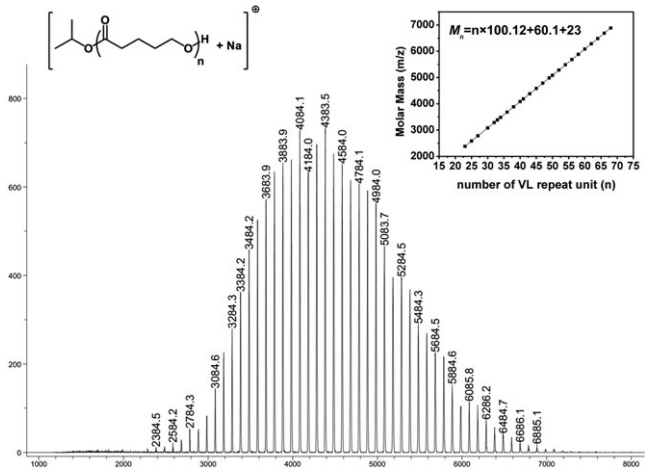

FIGURE 2 MALDI-TOF MS analysis for the resulting PVL by complex **3**/^{i}PrOH in toluene at 80°C ([M]/[I]/ROH = 200/1/1, $[M]_0 = 1.0$ M, $t = 60$ min)

moiety (d) and the aromatic ring belonging to the BnO-group (f) were found to be 3.56 ppm, 5.11 ppm and 7.35 ppm, respectively, indicating PVL macromolecular chains were capped with the hydroxyl group at one end and RO- group at the other end. The PVLs with low MW produced by complex **3**/^{i}PrOH or BnOH binary system (Table 3, entry 1; Table 4, entry 7) were tested by MALDI-TOF MS (Figure 2, and Figure S10 of ESI). All of the calculated masses were in agreement with the value of sodium-complexed linear PVL. The MALDI-TOF analysis indicated that there was no back-biting of the terminal active -O* to ester groups along the polymer chain, as evidenced by the absence of cyclic PVL (Figure 2), even when the polymerizations were carried out at high temperature (80°C). The MALDI-TOF also displayed BnO-capped PVL with narrow MWD, in

agreement with the ^{1}H-NMR spectrum (see Figure S10 of ESI). No cyclic PVLs were observed under the overloading of ROH (BnOH/[Mg] = 50). According to the extremely narrow MWD (M_w/M_n = 1.02), no transesterification side reactions were detected, in spite of ^{i}PrOH or BnOH as co-initiator. This ensured the reversible and fast chain transfer reaction and the immortal nature in the excess of ROH functioned as CTA again.

2.4 | Mechanism of investigation for ROP of δ-VL initiated by bis-ligated complexes/ROH system

The coordination-insertion and the activated monomer were two main mechanisms for the ROP of cyclic esters.[10,55–58] To explore the initiation and polymerization mechanism for complexes **1**–**3**, the interactions between monomer, Mg complexes and ROH (^{i}PrOH or BnOH) were investigated by *in situ* NMR at ambient temperature, respectively.

Generally, when the activated monomer mechanism is operative, monomer is directly coordinated to the metal center and activated by the complex, facilitating the subsequent attack by external alcohol. Coordination of monomer with metal complex will lead to peak shifts or occurrence of new resonances peaks in ^{1}H-NMR spectra.[10,56] In this work, no new resonance peaks or obvious chemical shifts were observed in ^{1}H-NMR spectra of complex **3**/δ-VL mixture, and the resonance peaks still kept intact when prolonging reaction time (see Figure S11 of ESI). As aforementioned, no polymers were obtained in the absence of ROH. This result strongly indicated that the bis-ligated complex alone had no interaction with monomer, excluding the possibility of activated monomer mechanism.[10,56,57]

Thus, ^{i}PrOH and BnOH were added to complex **3**, respectively, to testify the coordination-insertion mechanism. When 1 equiv. ^{i}PrOH was mixed with complex **3** in tol-d_8, the typical peaks of **L^{3}H** were detected, indicating the formation of proligands. Meanwhile, new resonances peaks at the range of 0.5–4.0 ppm were found (Figure 3). The new resonance peak that showed up at 3.03 ppm (Figure 3) was ascribed to methine of the isopropyl groups on the amine moiety of LMgO^{i}Pr. In addition, four characteristic peaks attributed to the methyls of isopropyl in complex **3** shifted from 0.24, 0.91, 0.96 and 1.11 ppm to 0.61, 1.07, 1.13 and 1.16 ppm. It was noteworthy that a new peak was detected at 0.92 ppm (f in Figure 3), corresponding to the methyl groups of ^{i}PrO- in alkoxides LMgO^{i}Pr. The integral areas of the alkoxide LMgO^{i}Pr to the generated proligand were almost 1:1. The same results were observed in the mixture of

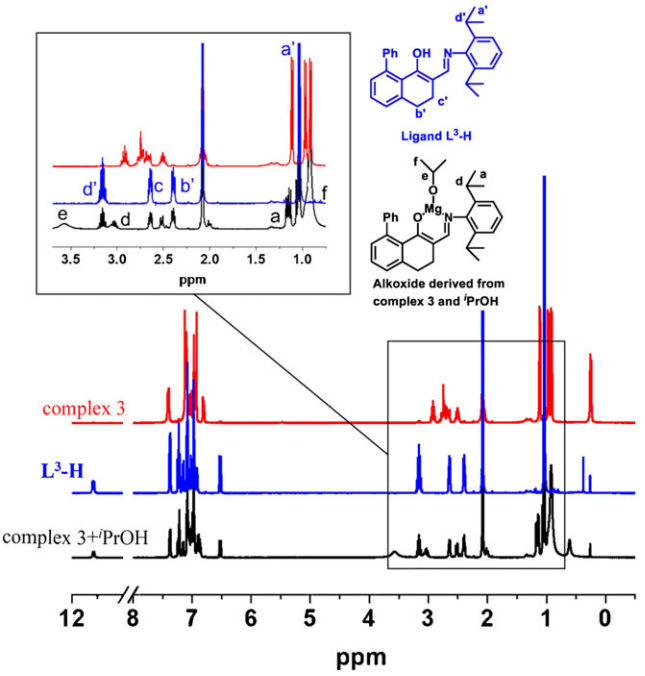

FIGURE 3 ^{1}H-NMR spectrum of the mixture of complex **3** and ^{i}PrOH in tol-d_8 (reaction for 12 min) compared with the spectra of complex **3** and ligand **L^3-H** (^{i}PrOH: [Mg] = 1:1)

complex **3** and 1 equiv. BnOH (see Figure S12 of ESI). Therefore, the reaction between complex **3** and 1 equiv. ROH produced 1 equiv. alkoxide complexes LMgOR (LMgO^{i}Pr or LMgOBn) as shown in equation 1, Scheme 3. And they were the real active species that can initiate the ROP of VL by inserting monomer into the metal-alkoxide bond.[55]

The reaction of complex **3** with different amounts of BnOH was also traced in C_6D_6 (Figure 4). Different from the mixture of complex **3** and BnOH with 1:1 molar ratio, the spectrum of the 1:2 mixture appeared a new broad peak near 4.3 ppm. This new resonance signal can be ascribed to the methene protons of inactive BnO- from Mg $(OBn)_2$ in equation 2. The same signal was observed in the mixture of Mg^{n}Bu$_2$ and 2 equiv. BnOH. This result indicated that the active alkoxides LMgOBn derived from equation 1 were not stable enough in excess of BnOH, leading to deactivation and transformation into simple alkoxides Mg $(OBn)_2$. According to the polymerization initiated by Mg^{n}Bu$_2$ under overloading of alcohol (see Table S2 of ESI), the Mg $(O^iPr)_2$ were evidently inactive species and Mg $(OBn)_2$ showed negligible activity, probably because of their different steric hindrance and lack of

$$L_2Mg + ROH \longrightarrow LMgOR + LH \quad (1)$$

$$LMgOR + ROH \longrightarrow Mg(OR)_2 + LH \quad (2)$$

SCHEME 3 The reaction equation between complex **3** and different amounts of BnOH

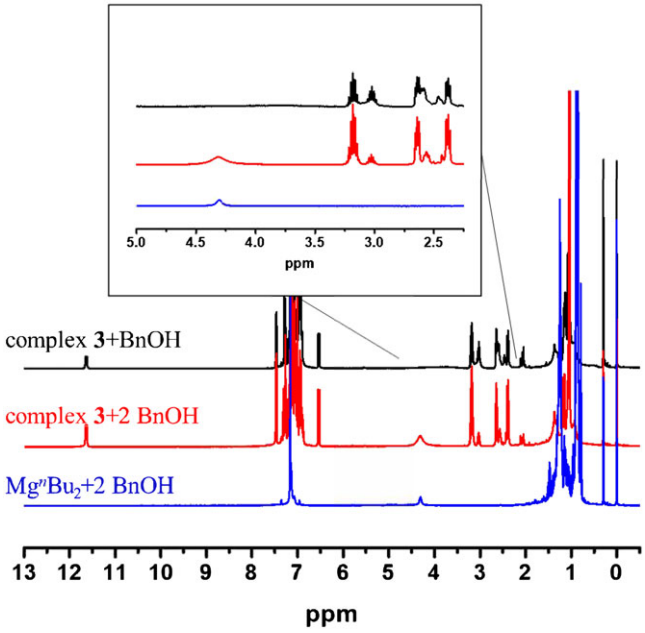

FIGURE 4 The reaction of complex **3** and 2 equiv. BnOH in C_6D_6, compared with the reaction of complex **3** with 1 equiv. BnOH and Mg^{n}Bu$_2$ with 2 equiv. BnOH (reaction time = 100 min)

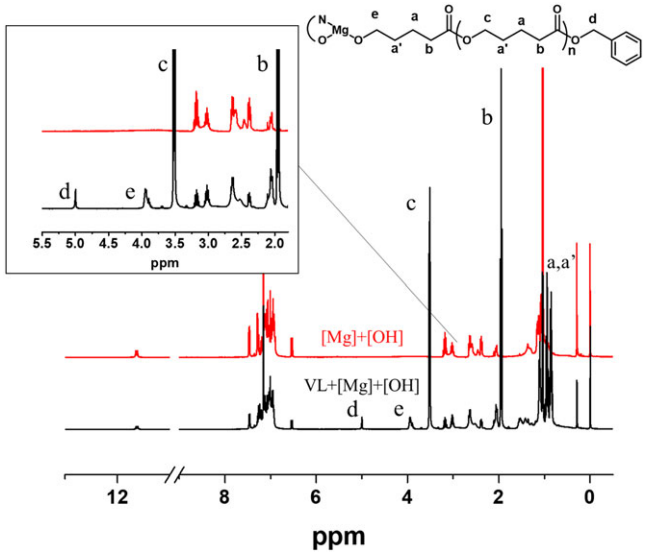

FIGURE 5 ^{1}H-NMR spectra of mixture of VL, complex **3** and BnOH in C_6D_6 at room temperature (VL:[Mg]:[OH] = 5:1:1), and the mixture of complex **3** and BnOH ([Mg]:[OH] = 1:1)

effective protection on the metal center. Nonetheless, complex **3** still maintained catalytic activity and worked well with excessive alcohol (even up to 50 equiv. BnOH). In combination with the results in Table 4, we could deduce that in the presence of monomer, the active magnesium alkoxide (LMgOR) still initiated ROP of δ-VL and produced active chains rapidly. The redundant alcohol actually functioned as an effective CTA instead of deactivating the active species, determining the MW of corresponding PVLs.

The influence of the different external alcohols on the stability of LMgOR was investigated. It was observed that the active alkoxides LMgO^{i}Pr decreased continuously in the presence of 2 equiv. ^{i}PrOH (see Figure S13 of ESI). All of the alkoxide complexes finally turned into proligands. The broad signal of methine proton in ^{i}PrO- shifted gradually from 3.63 ppm to 3.68 ppm. As the methine proton in ^{i}PrOH displayed a strong multiple peak at 3.70 ppm, it suggested the transformation from LMgO^{i}Pr into Mg $(O^iPr)_2$ as shown in equation 2, Scheme 3. This implied that the active alkoxides (LMgO^{i}Pr) were unstable in excess of ^{i}PrOH. By contrast, the active alkoxides derived from BnOH were apparently more stable. They still existed in excess of BnOH after 100 minutes, while the alkoxides from ^{i}PrOH were completely consumed at the same time. This was ascribed to the steric hindrance or the electronic effect of the BnO- group in alkoxide.

The reaction between complex **1** and 2 equiv. ^{i}PrOH was also explored, to test the steric effect of the ligand on the stability of the alkoxide (see Figure S14 of ESI). In sharp contrast, only the signal of proligands **L^{1}H** and no characteristic peaks of L^{1}MgO^{i}Pr were observed. This indicated that the LMgO^{i}Pr alkoxide derived from complex **1**, with the least steric bulk, was unstable and easy to transform into inactive alkoxide Mg $(O^iPr)_2$. Combining with the experimental results (Table 1, entries 5, 6, 18 and 19), it was convinced that the steric hindrance of alkoxide, LMgOR, including the steric bulk from the ancillary ligand segment (L) and the alcohol segment (RO-), can stabilize the active species effectively, resulting in higher apparent catalytic activity.

In order to gain more insight into the polymerization mechanism by alkoxides, a polymerization system with 5 equiv. VL, 1 equiv. complex **3** and 1 equiv. BnOH was tracked by ^{1}H-NMR spectra in C_6D_6 at room temperature (Figure 5). Besides the resonance signals of proligands, some new additional signals were found near the characteristic peaks of alkoxides LMgOBn, which could be assigned to the active chain LMg-$(VL)_n$-OBn. The methine in isopropyl groups of L segment in LMg- was detected at 3.02 ppm. Other newly formed signals that appeared at 5.00 ppm and 3.95 ppm, with 1:1 integral ratio, could be attributed to the CH_2- in BnO- group and CH_2- in LMg- group in the active chain end, respectively. It was deduced that during the ROP of δ-VL, the monomers inserted into the Mg-O bond in alkoxide and formed the active chain terminated by BnO- and LMg- groups. They only reduced 9.6% after 80 min, exhibiting good stability of the active chain (see Figure S15 of ESI).

Taking all into account, the coordination-insertion mechanism and immortal polymerization were strongly

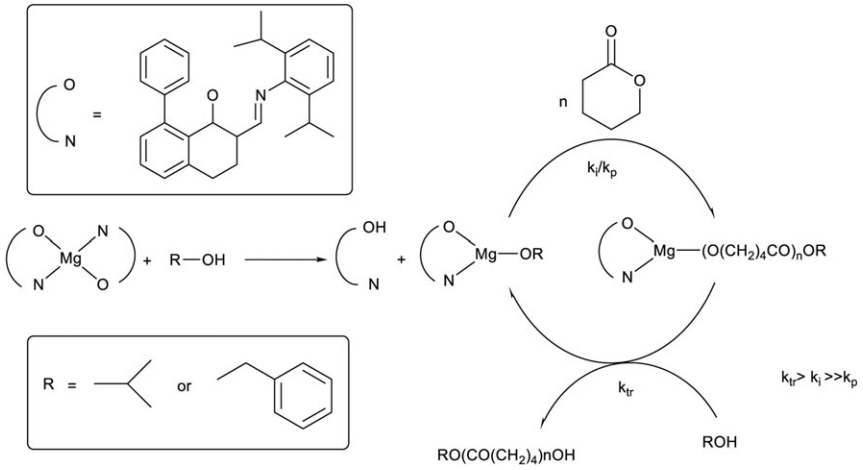

SCHEME 4 Proposed polymerization process and mechanism in ROP of δ-VL catalyzed by complex **3** and R-OH

presumed in the ROP of δ-VL initiated by homoleptic complex MgL_2, as shown in Scheme 4.[51,54] At first, the complexes reacted with ROH and turned into active alkoxide, LMgOR. Next, the monomer coordinated to Lewis acidic metal center, and then was attacked by RO-group, forming active chain ended with RO- and LMg-. The chain transfer rate and the initiation rate were much faster than the propagation rate, producing PVLs with ROH-dependent MW and consistently narrow MWD. According to the mechanism study, the stability of the alkoxide and active chains were basically dependent on the steric hindrance of organometallic complexes and alcohol.

3 | CONCLUSIONS

In conclusion, we developed a new series of bis-ligated, homoleptic magnesium complexes, displaying favorable catalytic activity toward ROP of L-LA, ε-CL and δ-VL. Remarkably, complex **3**, with the largest steric hindrance, exhibited excellent catalytic performance for the ROP of δ-VL. The MALDI-TOF analysis demonstrated that there was no transesterification side reaction, leading to the formation of linear PVL capped with RO- and hydroxy group. Moreover, complex **3** retained its high catalytic activity in excess of alcohol, affording PVLs with controlled MWs and consistently narrow MWD. It showed an immortal polymerization nature with rapid and reversible chain transfer during the polymerization. The monitoring of the polymerization process reflected a coordination-insertion mechanism by the magnesium alkoxides (LMgOR) derived from the reaction between the complex MgL_2 and ROH. It also manifested the effect of steric bulk on the stability of different alkoxides, explaining the maintained high catalytic activity under the overloading of alcohol. Above all, the new binary catalytic system combined with the homoleptic magnesium complex and alcohol was an efficient way to produce PVL with different MWs and quite narrow MWD.

ACKNOWLEDGEMENTS

The authors are grateful for financial support by the National Natural Science Foundation of China (No. 21474100).

ORCID

Bin Wang https://orcid.org/0000-0002-3130-3229
Yue-Sheng Li https://orcid.org/0000-0003-4637-4254

REFERENCES

[1] G. L. Gregory, E. M. Lopez-Vidal, A. Buchard, *Chem. Commun.* **2017**, *53*, 2198.

[2] Y. Zhu, C. Romain, C. K. Williams, *Nature* **2016**, *540*, 354.

[3] D. K. Schneiderman, M. A. Hillmyer, *Macromolecules* **2017**, *50*, 3733.

[4] V. H. Sangeetha, H. Deka, T. O. Varghese, S. K. Nayak, *Polym. Compos.* **2018**, *39*, 81.

[5] X. Zhang, M. Fevre, G. O. Jones, R. M. Waymouth, *Chem. Rev.* **2018**, *118*, 839.

[6] H.-Y. Ji, B. Wang, L. Pan, Y.-S. Li, *Green Chem.* **2018**, *20*, 641.

[7] S. M. Guillaume, E. Kirillov, Y. Sarazin, J. F. Carpentier, *Chem. Eur. J.* **2015**, *21*, 7988.

[8] E. Stirling, Y. Champouret, M. Visseaux, *Polym. Chem.* **2018**, *9*, 2517.

[9] M. Labet, W. Thielemans, *Chem. Soc. Rev.* **2009**, *38*, 3484.

[10] I. D'Auria, C. Tedesco, M. Mazzeo, C. Pellecchia, *Dalton Trans.* **2017**, *46*, 12217.

[11] S. Dagorne, M. Normand, E. Kirillov, J.-F. Carpentier, *Coordin. Chem. Rev.* **2013**, *257*, 1869.

[12] S. Dagorne, C. Fliedel, *Top. Organomet. Chem.* **2013**, *41*, 125.

[13] J. Wojtaszak, K. Mierzwicki, S. Szafert, N. Gulia, J. Ejfler, *Dalton Trans.* **2014**, *43*, 2424.

[14] C. S. Hege, S. M. Schiller, *Green Chem.* **2014**, *16*, 1410.

[15] S. P. Parwe, S. D. Warkad, M. V. Mane, P. S. Shedage, B. Garnaik, *Polymer* **2017**, *111*, 244.

[16] C. Duval, C. Nouvel, J.-L. Six, *J. Polym. Sci., Part a: Polym. Chem.* **2014**, *52*, 1130.

[17] C. Exley, *Morphologie* **2016**, *100*, 51.

[18] I. E. Nifant'ev, A. V. Shlyakhtin, V. V. Bagrov, M. E. Minyaev, A. V. Churakov, S. G. Karchevsky, K. P. Birin, P. V. Ivchenko, *Dalton Trans.* **2017**, *46*, 12 132.

[19] A. Garcés, L. F. Sánchez-Barba, J. Fernández-Baeza, A. Otero, A. Lara-Sánchez, A. M. Rodríguez, *Organometallics* **2017**, *36*, 884.

[20] J. Hu, C. Kan, H. Wang, H. Ma, *Macromolecules* **2018**, *51*, 5304.

[21] I. E. Nifant'ev, A. V. Shlyakhtin, A. N. Tavtorkin, P. V. Ivchenko, R. S. Borisov, A. V. Churakov, *Catal. Commun.* **2016**, *87*, 106.

[22] I. E. Nifant'ev, A. V. Shlyakhtin, V. V. Bagrov, P. D. Komarov, M. A. Kosarev, A. N. Tavtorkin, M. E. Minyaev, V. A. Roznyatovsky, P. V. Ivchenko, *Polym. Chem.* **2017**, *8*, 6806.

[23] T. Rosen, I. Goldberg, W. Navarra, V. Venditto, M. Kol, *Angew. Chem. Int. Ed.* **2018**, *57*, 7191.

[24] H. Wang, J. Guo, Y. Yang, H. Ma, *Dalton Trans.* **2016**, *45*, 10 942.

[25] Y. Yang, H. Wang, H. Ma, *Polyhedron* **2016**, *117*, 569.

[26] N. Romero, Q. Dufrois, L. Vendier, C. Dinoi, M. Etienne, *Organometallics* **2017**, *36*, 564.

[27] D. Jedrzkiewicz, D. Kantorska, J. Wojtaszak, J. Ejfler, S. Szafert, *Dalton Trans.* **2017**, *46*, 4929.

[28] C. Kan, J. Hu, Y. Huang, H. Wang, H. Ma, *Macromolecules* **2017**, *50*, 7911.

[29] M. Keram, H. Ma, *Appl. Organomet. Chem.* **2017**, *31*, e3893.

[30] K. S. Kwon, S. Nayab, H.-I. Lee, J. H. Jeong, *Polyhedron* **2017**, *126*, 127.

[31] S. Mantri, A. Routaray, N. Nath, K. Sutar Alekha, T. Maharana, *Polym. Int.* **2016**, *66*, 313.

[32] A. Otero, J. Fernandez-Baeza, L. F. Sanchez-Barba, S. Sobrino, A. Garces, A. Lara-Sanchez, A. M. Rodriguez, *Dalton Trans.* **2017**, *46*, 15 107.

[33] D. Jędrzkiewicz, G. Adamus, M. Kwiecień, Ł. John, J. Ejfler, *Inorg. Chem.* **2017**, *56*, 1349.

[34] R. Duan, C. Hu, X. Li, X. Pang, Z. Sun, X. Chen, X. Wang, *Macromolecules* **2017**, *50*, 9188.

[35] C. Gallegos, V. Tabernero, F. M. García-Valle, M. E. G. Mosquera, T. Cuenca, J. Cano, *Organometallics* **2013**, *32*, 6624.

[36] Y. Huang, X. Kou, Y. L. Duan, F. F. Ding, Y. F. Yin, W. Wang, Y. Yang, *Dalton Trans.* **2018**, *47*, 8121.

[37] K. A. Gerling, N. M. Rezayee, A. L. Rheingold, D. B. Green, J. M. Fritsch, *Dalton Trans.* **2014**, *43*, 16 498.

[38] C. A. Wheaton, P. G. Hayes, B. J. Ireland, *Dalton Trans.* **2009**, *25*, 4832.

[39] C. Fliedel, V. Rosa, F. M. Alves, A. M. Martins, T. Avilés, S. Dagorne, *Dalton Trans.* **2015**, *44*, 12 376.

[40] J. Ejfler, S. Szafert, K. Mierzwicki, L. B. Jerzykiewicz, P. Sobota, *Dalton Trans.* **2008**, *46*, 6556.

[41] M. Huang, C. Pan, H. Ma, *Dalton Trans.* **2015**, *44*, 12 420.

[42] R. Petrus, P. Sobota, *Organometallics* **2012**, *31*, 4755.

[43] S. Song, X. Zhang, H. Ma, Y. Yang, *Dalton Trans.* **2012**, *41*, 3266.

[44] C. C. Roberts, B. R. Barnett, D. B. Green, J. M. Fritsch, *Organometallics* **2012**, *31*, 4133.

[45] H.-J. Chuang, H.-L. Chen, B.-H. Huang, T.-E. Tsai, P.-L. Huang, T.-T. Liao, C.-C. Lin, *J. Polym. Sci., Part a: Polym. Chem.* **2012**, *51*, 1185.

[46] V. Poirier, T. Roisnel, J. F. Carpentier, Y. Sarazin, *Dalton Trans.* **2011**, *40*, 523.

[47] Z.-R. Dai, C.-F. Yin, C. Wang, J.-C. Wu, *Chinese Chem. Lett.* **2016**, *27*, 1649.

[48] B. Raghavendra, K. Bakthavachalam, B. Ramakrishna, N. Dastagiri Reddy, *Organometallics* **2017**, *36*, 4005.

[49] B. Raghavendra, P. V. S. Shashank, M. K. Pandey, N. D. Reddy, *Organometallics* **2018**, *37*, 1656.

[50] D.-P. Song, Y.-X. Wang, H.-L. Mu, B.-X. Li, Y.-S. Li, *Organometallics* **2011**, *30*, 925.

[51] K. A. Frazier, R. D. Froese, Y. He, J. Klosin, C. N. Theriault, P. C. Vosejpka, Z. Zhou, K. A. Abboud, *Organometallics* **2011**, *30*, 3318.

[52] S. Naumann, D. Wang, *Macromolecules* **2016**, *49*, 8869.

[53] N. Ajellal, J. F. Carpentier, C. Guillaume, S. M. Guillaume, M. Helou, V. Poirier, Y. Sarazin, A. Trifonov, *Dalton Trans.* **2010**, *39*, 8363.

[54] C. K. Williams, L. E. Breyfogle, S. K. Choi, W. Nam, V. G. Young, M. A. Hillmyer, W. B. Tolman, *J. Am. Chem. Soc.* **2003**, *125*, 11 350.

[55] V. Poirier, T. Roisnel, J. F. Carpentier, Y. Sarazin, *Dalton Trans.* **2009**, *44*, 9820.

[56] Y. Sun, Y. Cui, J. Xiong, Z. Dai, N. Tang, J. Wu, *Dalton Trans.* **2015**, *44*, 16 383.

[57] C. Bakewell, A. J. P. White, N. J. Long, C. K. Williams, *Inorg. Chem.* **2013**, *52*, 12 561.

[58] T. Rosen, I. Goldberg, V. Venditto, M. Kol, *J. Am. Chem. Soc.* **2016**, *138*, 12 041.

SUPPORTING INFORMATION

Additional supporting information may be found online in the Supporting Information section at the end of the article.

How to cite this article: Chen X-L, Wang B, Pan L, Li Y-S. Homoleptic, bis-ligated magnesium complexes for ring-opening polymerization of lactide and lactones: Synthesis, structure, polymerization behavior and mechanism studies. *Appl Organometal Chem*. 2019;e4770. https://doi.org/10.1002/aoc.4770